

Diene derivatives of hexarhodium hexadecacarbonyl. Molecular structures of $\text{Rh}_6(\text{CO})_{14}(\eta^4\text{-CH}_2\text{C}(\text{Me})\text{C}(\text{Me})\text{CH}_2)$ and $\text{Rh}_6(\text{CO})_{12}(\eta^4\text{-CH}_2\text{C}(\text{Me})\text{C}(\text{Me})\text{CH}_2)_2$, and their substitution reactions with bis(diphenylphosphino)methane

Zhaomin Hou, Yasuo Wakatsuki and Hiroshi Yamazaki

The Institute of Physical and Chemical Research (RIKEN), Wako-Shi, Saitama 351-01 (Japan)

(Received June 15th, 1990)

Abstract

Reaction of $\text{Rh}_4(\text{CO})_{12}$ with 2,3-dimethyl-1,3-butadiene (DMBD) in refluxing hexane gives $\text{Rh}_6(\text{CO})_{14}(\eta^4\text{-CH}_2\text{C}(\text{Me})\text{C}(\text{Me})\text{CH}_2)$ (**1**) and $\text{Rh}_6(\text{CO})_{12}(\eta^4\text{-CH}_2\text{C}(\text{Me})\text{C}(\text{Me})\text{CH}_2)_2$ (**2**), both of which have been characterized by X-ray crystallography. Complex **1** crystallizes in the orthorhombic space group $P2_12_12_1$ with a 14.430(3), b 16.970(3), c 10.908(2) Å, and $Z = 4$. Refinement converged to $R = 0.0425$ and $R_w = 0.0409$ based on 2511 unique observations (NO) and 362 parameters varied (NV). The molecule consists of an octahedral cluster of rhodium atoms, bearing ten terminal and four face bridging carbonyl groups and a DMBD ligand coordinated to one Rh atom in $\eta^4\text{-s-cis}$ form. The crystal data for **2** are as follows: monoclinic space group Cc , a 17.636(2), b 9.561(1), c 18.234(4) Å, β 97.24(1)°, $Z = 4$, $R = 0.0286$, $R_w = 0.0317$, $NO = 2929$, and $NV = 380$. Complex **2** has a similar structure as **1**, and the two DMBD ligands are coordinated to two rhodium apices which are mutually *trans* to each other in the octahedral skeleton. Although the coordination of the DMBD ligands in **2** is rigid at room temperature, their rotation is observed at elevated temperatures, (activation energy E_a 9.7 kcal mol⁻¹). Reactions of **1** and **2** with bis(diphenylphosphino)methane (DPPM) take place rapidly at room temperature to give $\text{Rh}_6(\text{CO})_{14}(\text{DPPM})$ and $\text{Rh}_6(\text{CO})_{12}(\text{DPPM})_2$ respectively. These reactions are much faster than the similar reaction of $\text{Rh}_6(\text{CO})_{16}$. The reaction of **1** with DPPM has been found to be two to three times faster than that of **2**, indicating that ligands attached to a metal apex can affect the rate of substitution occurring even at the remotest apex of the octahedron.

Introduction

Hexadecacarbonylrhodium derivatives $\text{Rh}_6(\text{CO})_{16-n}\text{L}_n$, bearing ligands L which are more easily displaced than carbon monoxide, are of much interest as potential cluster catalysts for a series of hydrocarbon reactions such as hydrogenation [1*].

* A reference number with an asterisk indicates a note in the list of references.

Moreover, such derivatives are expected to have better solubility compared with the parent $\text{Rh}_6(\text{CO})_{16}$ which is insoluble in most of the common solvents. Open chain dienes are suitable ligands in this regard, as they are relatively labile and provide two accessible coordination sites on liberation. Clusters with diene ligands are also of structural interest since the ligands can have various coordination forms [2]. Up to now, a few diene complexes of rhodium carbonyl clusters have been known, but none has been well characterized [3*]. We have recently obtained and structurally characterized the hexarhodium carbonyl cluster bearing two diene ligands, $\text{Rh}_6(\text{CO})_{12}(\eta^4\text{-CH}_2\text{C}(\text{Me})\text{C}(\text{Me})\text{CH}_2)_2$. Its precursor, $\text{Rh}_6(\text{CO})_{14}(\eta^4\text{-CH}_2\text{C}(\text{Me})\text{C}(\text{Me})\text{CH}_2)$ [3a], has also been studied by X-ray crystallography. These clusters have good solubility in common solvents and easy displacement of the diene ligand has been demonstrated by the reaction with bis(diphenylphosphino)methane (DPPM). We report here the structures of these two diene clusters and their reactions with DPPM.

Results and discussion

The mono-diene complex, $\text{Rh}_6(\text{CO})_{14}(\eta^4\text{-CH}_2\text{C}(\text{Me})\text{C}(\text{Me})\text{CH}_2)$ (**1**) was previously reported to be obtained by refluxing a 1:20 mixture of $\text{Rh}_4(\text{CO})_{12}$ and 2,3-dimethyl-1,3-butadiene (DMBD) in hexane followed by column chromatography [3a]. We have carried out a similar reaction and by examining the reaction mixture carefully found that the bis-diene complex, $\text{Rh}_6(\text{CO})_{12}(\eta^4\text{-CH}_2\text{C}(\text{Me})\text{C}(\text{Me})\text{CH}_2)_2$ (**2**) was also formed besides **1**. These two complexes were separated by repeated recrystallization. Reflux of **1** with DMBD in hexane also gave **2**. Accordingly, complex **2** is thought to be formed via **1** and not by the direct reaction of the starting $\text{Rh}_4(\text{CO})_{12}$ with DMBD. Both clusters have good solubility in benzene, acetone, tetrahydrofuran and methylene dichloride. Complex **2** is soluble even in hexane.

Structure. The molecular structure of **1** is depicted in Fig. 1. The positional parameters, bond lengths, and selected bond angles are listed in Tables 1–3. The molecule consists of an octahedral cluster of rhodium atoms, bearing ten terminal and four face-bridging carbonyl groups and one DMBD ligand. The diene ligand is coordinated to Rh(5) in η^4 -*s-cis* form.

The average metal–metal bond length is 2.773 Å, comparable with that (2.776 Å) found in $\text{Rh}_6(\text{CO})_{16}$ [4]. The average Rh–C (1.93 Å) and C–O (1.13 Å) bond lengths for terminal carbonyls are, as expected, shorter than those (Rh–C: 2.20, C–O: 1.17 Å) for bridging carbonyls respectively. In contrast to what happens in rhodium clusters with phosphorus ligands [5], the introduction of a diene to the cluster resulted in no significant change in Rh–C bond lengths for bridging carbonyls. In complex **1** the mean bond distance (2.20 Å) between Rh(5), which bears the DMBD ligand, and the μ_3 -carbonyl carbons, C(1,4), is almost equal to that (2.19 Å) of Rh(1,2,6,4)–C(1,4) and Rh(3)–C(2,3).

The average Rh–C bond length for Rh(5)–DMBD is 2.20 Å, which coincides with the corresponding value in the mononuclear rhodium complex of 1,3-butadiene, $(\text{C}_4\text{H}_6)_2\text{RhCl}$ [6]. The plane formed by C(51,52,53,54) is not parallel to that of Rh(1,2,6,4). The dihedral angle between them is $17.2(9)^\circ$, with C(52,53) away from the rhodium basal plane.

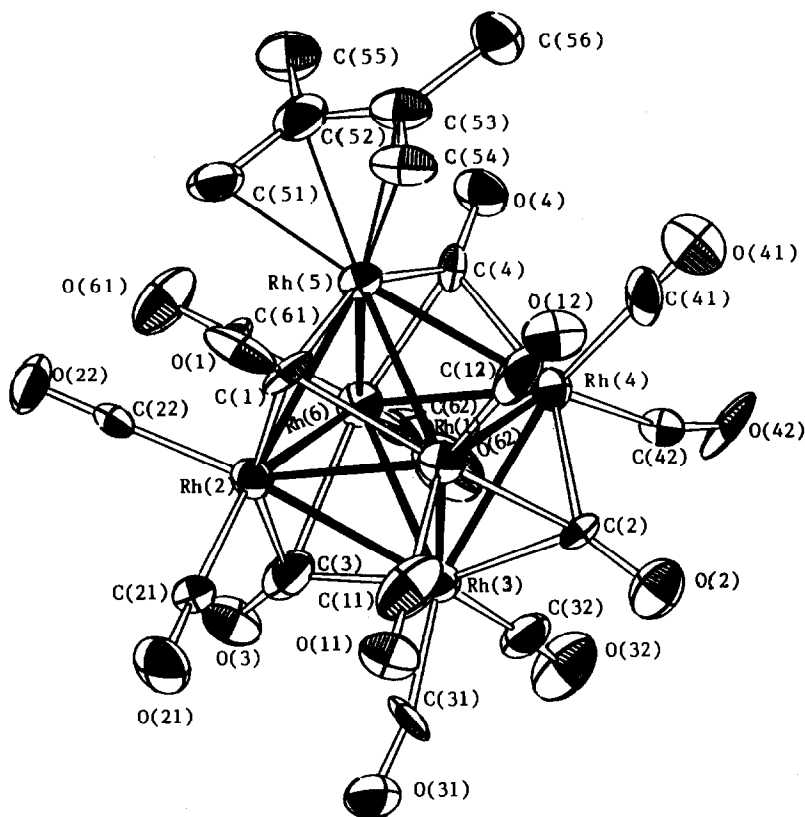


Fig. 1. ORTEP drawing of 1. The H atoms are omitted for clarity.

Figure 2 shows the molecular structure and numbering scheme of 2. The positional parameters, bond lengths, and selected angles are listed in Tables 4–6. The overall structure and bond lengths of 2 are similar to those of 1. The average Rh–Rh bond length is 2.774 Å. The average Rh–C and C–O bond lengths are 1.91 and 1.12 Å, respectively, for the terminal carbonyls, and 2.17 and 1.19 Å, respectively, for the face-bridging carbonyl groups.

Complex 2 has a mean Rh–C (DMBD) bond distance of 2.21 Å. The two DMBD are coordinated to two apices (Rh(1) and Rh(6)) of the rhodium octahedron, which are mutually *trans*. As shown in Fig. 2, the upper half of the rhodium octahedron has four triangular faces, of which two bear the μ_3 -carbonyl ligand. The DMBD coordinates to Rh(1) in such a manner that it is bisected by the plane defined by Rh(1) and the two μ_3 -carbonyl carbons, C(1) and C(2). The situation holds true for the lower half, and since the plane formed by Rh(6), C(3) and C(4) meets the plane defined by Rh(1), C(1) and C(2) at a right angle, and the two diene moieties in 2 are twisted away from each other by 90° around the axis of Rh(1)–Rh(6). This stereochemistry is formally obtained when all four terminal CO groups on the two *trans* Rh atoms in $\text{Rh}_6(\text{CO})_{16}$ are replaced with two DMBD. Plane Rh(2,3,4,5) forms dihedral angles of 19.5(7) and 18.7(7)° with planes C(11,12,13,14) and C(61,62,63,64), respectively. The dihedral angle between these two DMBD planes is 28.3(8)°.

Table 1

Fractional coordinates ($\times 10^4$) of the non-hydrogen atoms of **1** and isotropic thermal parameters (esd's in parentheses)

Atom	x	y	z	$U_{eq}, \text{\AA}^2$
Rh(1)	5957(1)	2059(1)	3823(1)	2.3(0.0)
Rh(2)	4035(1)	2062(1)	3829(1)	2.1(0.0)
Rh(3)	4994(4)	1096(1)	5423(1)	2.3(0.0)
Rh(4)	5973(1)	470(1)	3490(1)	2.1(0.0)
Rh(5)	4963(3)	1417(1)	1825(1)	1.9(0.0)
Rh(6)	4024(1)	473(1)	3481(1)	2.3(0.0)
O(1)	5014(21)	3214(5)	2062(10)	3.5(0.3)
O(2)	7153(10)	1078(8)	5706(13)	3.7(0.4)
O(3)	2866(9)	1105(8)	5669(12)	3.4(0.4)
O(4)	4915(29)	-424(6)	1377(10)	3.1(0.4)
O(11)	6138(11)	3405(8)	5645(13)	4.1(0.4)
O(12)	7670(9)	2539(8)	2359(11)	3.2(0.4)
O(21)	3915(11)	3490(8)	5521(14)	4.5(0.4)
O(22)	2296(15)	2469(14)	2440(20)	4.0(0.7)
O(31)	4844(19)	2251(7)	7560(11)	3.9(0.6)
O(32)	4938(34)	-430(7)	6886(12)	5.1(0.5)
O(41)	7725(10)	577(8)	1938(14)	4.4(0.4)
O(41)	7725(10)	577(8)	1938(14)	4.4(0.4)
O(61)	2243(10)	470(10)	2107(14)	5.0(0.5)
O(62)	3561(12)	-1154(8)	4685(15)	5.2(0.5)
C(1)	4978(30)	2594(8)	2526(13)	2.6(0.4)
C(2)	6534(11)	1149(9)	4965(14)	1.7(0.4)
C(3)	3536(15)	1142(11)	5186(17)	3.4(0.5)
C(4)	4895(26)	94(8)	2098(13)	2.0(0.5)
C(11)	6098(17)	2936(15)	4994(22)	5.0(0.7)
C(12)	7096(16)	2354(11)	2833(20)	4.1(0.6)
C(21)	3945(12)	2956(9)	4866(14)	1.6(0.4)
C(22)	2949(12)	2311(10)	2976(15)	2.2(0.4)
C(31)	5010(32)	1814(10)	6788(14)	4.2(0.5)
C(32)	5041(43)	144(10)	6352(14)	3.2(0.5)
C(41)	7061(14)	476(11)	2508(20)	3.6(0.6)
C(42)	6196(12)	-600(9)	4292(14)	1.8(0.4)
C(61)	2939(13)	540(11)	2569(15)	2.5(0.5)
C(62)	3684(15)	-515(12)	4032(16)	3.2(0.5)
C(51)	4031(14)	1868(11)	427(18)	3.6(0.5)
C(52)	4494(13)	1221(11)	-57(18)	3.4(0.5)
C(53)	5507(13)	1217(11)	-53(18)	3.3(0.5)
C(54)	5950(14)	1884(11)	418(18)	3.5(0.5)
C(55)	3949(14)	528(11)	-571(17)	3.6(0.5)
C(56)	6064(14)	527(11)	-575(17)	3.6(0.5)

^1H NMR and IR spectra of **1** and **2** are in good agreement with their crystal structures. ^1H NMR spectrum of **2** in CDCl_3 shows signals at 3.55 (d, J 1.2 Hz, 2 H), 2.18(s, 6H) and 1.56(br s, 2H) ppm [7*]. The peaks at 3.55 and 1.56 ppm are the typical pattern of terminal vinyl protons in an η^4 -coordinated *s-cis*-1,3-butadiene, i.e. the lower field and higher field absorptions are respectively attributable to the *syn* and *anti* protons, respectively, relative to the methyl groups [8]. The ^1H NMR spectrum of **2** is similar to that of **1**. However, since the two DMBD in **2** are oriented in different directions, no equivalent hydrogen atoms are present in the

Table 2

Bond lengths of the non-hydrogen atoms of **1** (esd's in parentheses)

Rh(1)–Rh(2)	2.774(2)	Rh(1)–C(12)	2.03(2)
Rh(1)–Rh(3)	2.766(3)	Rh(2)–C(21)	1.90(2)
Rh(1)–Rh(4)	2.721(2)	Rh(2)–C(2)	1.87(2)
Rh(1)–Rh(5)	2.827(3)	Rh(3)–C(31)	1.92(2)
Rh(2)–Rh(3)	2.761(3)	Rh(3)–C(32)	1.91(2)
Rh(2)–Rh(5)	2.787(3)	Rh(4)–C(41)	1.90(2)
Rh(2)–Rh(6)	2.723(2)	Rh(4)–C(42)	2.04(2)
Rh(3)–Rh(4)	2.752(3)	Rh(6)–C(61)	1.86(2)
Rh(3)–Rh(6)	2.750(3)	Rh(6)–C(62)	1.85(2)
Rh(4)–Rh(5)	2.829(3)	Rh(5)–C(51)	2.17(2)
Rh(4)–Rh(6)	2.813(2)	Rh(5)–C(52)	2.19(2)
Rh(5)–Rh(6)	2.769(3)	Rh(5)–C(53)	2.22(2)
Rh(1)–C(1)	2.20(3)	Rh(5)–C(54)	2.24(2)
Rh(2)–C(1)	2.17(3)	C(1)–O(1)	1.17(2)
Rh(5)–C(1)	2.14(1)	C(2)–O(2)	1.21(2)
Rh(1)–C(2)	2.15(2)	C(3)–O(3)	1.10(2)
Rh(3)–C(2)	2.28(2)	C(4)–O(4)	1.18(2)
Rh(4)–C(2)	2.14(2)	C(11)–O(11)	1.07(3)
Rh(2)–C(3)	2.27(2)	C(12)–O(12)	1.03(3)
Rh(3)–C(3)	2.12(2)	C(21)–O(21)	1.15(2)
Rh(6)–C(3)	2.29(2)	C(22)–O(22)	1.14(3)
Rh(4)–C(4)	2.27(3)	C(31)–O(31)	1.15(2)
Rh(5)–C(4)	2.27(1)	C(32)–O(32)	1.14(2)
Rh(6)–C(4)	2.07(3)	C(41)–O(41)	1.17(3)
Rh(1)–C(11)	1.97(2)	C(42)–O(42)	0.99(2)
C(61)–O(61)	1.13(2)	C(52)–C(55)	1.52(3)
C(62)–O(62)	1.31(2)	C(53)–C(54)	1.40(3)
C(51)–C(52)	1.39(3)	C(53)–C(56)	1.53(3)
C(52)–C(53)	1.46(3)		

Table 3

Selected bond angles of the non-hydrogen atoms of **1** (esd's in parentheses)

Rh(1)–C(1)–Rh(2)	79.1(5)	Rh(4)–C(4)–Rh(5)	77.2(7)
Rh(1)–C(1)–Rh(5)	81.5(8)	Rh(4)–C(4)–Rh(6)	80.8(5)
Rh(2)–C(1)–Rh(5)	80.7(8)	Rh(5)–C(4)–Rh(6)	79.3(6)
Rh(1)–C(1)–O(1)	129(3)	Rh(4)–C(4)–O(4)	130(3)
Rh(2)–C(1)–O(1)	133(3)	Rh(5)–C(4)–O(4)	130(1)
Rh(5)–C(1)–O(1)	133(1)	Rh(6)–C(4)–O(4)	137(3)
Rh(1)–C(2)–Rh(3)	77.2(5)	C(11)–Rh(1)–C(12)	94.4(9)
Rh(1)–C(2)–Rh(4)	78.8(5)	C(21)–Rh(2)–C(22)	93.3(7)
Rh(3)–C(2)–Rh(4)	77.0(5)	C(31)–Rh(3)–C(32)	97.2(7)
Rh(1)–C(2)–O(2)	138(1)	C(41)–Rh(4)–C(42)	96.7(8)
Rh(3)–C(2)–O(2)	125(1)	C(61)–Rh(6)–C(62)	90.4(8)
Rh(4)–C(2)–O(2)	137(1)	C(51)–C(52)–C(53)	119(2)
Rh(2)–C(3)–Rh(3)	77.9(7)	C(51)–C(52)–C(55)	121(2)
Rh(2)–C(3)–Rh(6)	73.3(6)	C(53)–C(52)–C(55)	121(2)
Rh(3)–C(3)–Rh(6)	77.0(7)	C(52)–C(53)–C(54)	117(2)
Rh(2)–C(3)–O(3)	129(2)	C(52)–C(53)–C(56)	122(2)
Rh(3)–C(3)–O(3)	144(2)	C(54)–C(53)–C(56)	121(2)
Rh(6)–C(3)–O(3)	129(2)		

DMBD moiety except for the protons within the same methyl group. Consequently, six peaks are observed in its ^1H NMR spectrum: 3.68 (d, J 1.2 Hz, 2H), 3.65(d, J 1.2 Hz, 2 H), 2.20 (s, 6 H), 2.19(s, 6 H), 1.62(br s, 2 H), 1.59 (br s, 2 H) ppm in CDCl_3 . The IR spectra of both **1** and **2** show strong absorptions at 2000–2150 and 1760–1790 cm^{-1} , due to terminal and face bridging carbonyl groups, respectively. The structure of **2** in solution is rigid at room temperature, but at elevated

Table 4

Fractional coordinates ($\times 10^4$) of the non-hydrogen atoms of **2** and isotropic thermal parameters (esd's in parentheses)

Atom	<i>x</i>	<i>y</i>	<i>z</i>	$U_{\text{eq}}, \text{\AA}^2$
Rh(1)	9322(0)	2149(1)	4463(0)	2.1(0.0)
Rh(2)	9593(0)	2166(1)	6017(0)	2.2(0.0)
Rh(3)	10228(2)	4174(1)	5235(2)	2.4(0.0)
Rh(4)	10909(0)	2163(1)	4472(0)	2.2(0.0)
Rh(5)	10252(2)	131(1)	5233(2)	2.2(0.0)
Rh(6)	11172(0)	2160(1)	6008(0)	2.2(0.0)
O(1)	8526(5)	4499(10)	5270(5)	4.0(0.3)
O(2)	10049(5)	−215(9)	3557(4)	3.2(0.2)
O(3)	12011(5)	4363(11)	5184(5)	5.0(0.3)
O(4)	10452(5)	−202(10)	6921(5)	4.1(0.3)
O(21)	8160(6)	735(14)	6382(6)	6.4(0.4)
O(22)	9601(7)	3827(14)	7422(6)	7.4(0.4)
O(31)	10132(7)	6442(11)	4064(5)	6.4(0.4)
O(32)	10430(8)	6409(11)	6426(6)	7.5(0.5)
O(41)	10876(7)	3927(13)	3080(6)	6.5(0.4)
O(42)	12375(6)	748(15)	4177(6)	7.6(0.5)
O(51)	11563(7)	−1977(11)	5237(8)	7.3(0.4)
O(52)	8955(6)	−1905(12)	5263(6)	5.7(0.4)
C(1)	9051(7)	3836(12)	5231(6)	2.9(0.3)
C(2)	10095(6)	559(14)	4063(6)	2.7(0.3)
C(3)	11475(6)	3550(13)	5219(6)	2.7(0.3)
C(4)	10399(7)	512(12)	6379(7)	3.0(0.3)
C(21)	8663(7)	1233(15)	6207(7)	3.4(0.4)
C(22)	9600(7)	3228(14)	6901(7)	3.4(0.4)
C(31)	10146(8)	5532(13)	4474(7)	3.4(0.4)
C(32)	10342(9)	5600(16)	5992(7)	4.8(0.5)
C(41)	10852(8)	3231(16)	3590(7)	4.1(0.4)
C(42)	11801(7)	1197(17)	4294(7)	4.1(0.4)
C(51)	11080(7)	−1238(13)	5251(7)	3.2(0.3)
C(52)	9430(8)	−1122(14)	5264(7)	3.8(0.4)
C(11)	8793(7)	3659(15)	3634(7)	3.6(0.4)
C(12)	8724(6)	2287(15)	3340(6)	3.3(0.3)
C(13)	8353(6)	1206(15)	3741(7)	3.6(0.4)
C(14)	8097(7)	1555(18)	4415(7)	4.4(0.4)
C(15)	9036(8)	1927(17)	2612(7)	4.4(0.4)
C(16)	8276(9)	−277(16)	3466(9)	5.0(0.5)
C(61)	12396(7)	1667(18)	6077(7)	4.3(0.4)
C(62)	12132(7)	1245(16)	6748(7)	3.6(0.4)
C(63)	11776(6)	2273(15)	7153(6)	3.1(0.3)
C(64)	11698(7)	3610(15)	6861(7)	3.7(0.4)
C(65)	12234(9)	−337(18)	7015(9)	5.8(0.5)
C(66)	11454(8)	1921(17)	7888(7)	4.2(0.4)

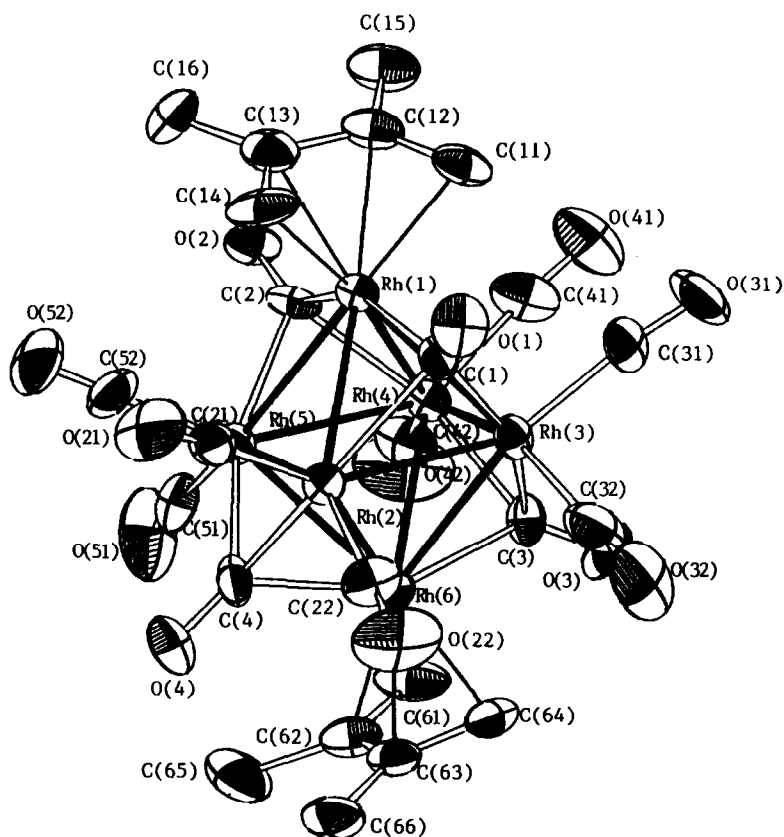


Fig. 2. ORTEP drawing of **2**. The H atoms are omitted for clarity.

temperatures it becomes fluxional. Figure 3 shows the variable temperature ^1H NMR spectra of **2** in C_6D_6 . The chemical shifts between the two *syn* vinyl proton resonances (3.51 and 3.47 ppm), the two *anti* vinyl proton resonances (1.48 and 1.44 ppm) and the two methyl proton resonances (1.80 and 1.78 ppm) decrease gradually as the temperature is raised. The resonances of the vinyl and the methyl protons coalesced at 65°C and 55°C , respectively, indicating that the rotation of the two dienes around the Rh(1)–Rh(6) axis occurred. The calculated activation energy E_a was 9.7 kcal mol^{-1} [9*].

Reaction with DPPM. The diene ligands in **1** and **2** can be readily replaced by bis(diphenylphosphino)methane (DPPM). Both reactions were much faster than the similar substitution of carbonyl groups in $\text{Rh}_6(\text{CO})_{16}$ where completion of the reaction requires 20–40 hours. [10] On addition of one equiv. of DPPM to CD_2Cl_2 solution of **1**, the ^1H NMR signals of the coordinated DMBD disappeared immediately and new peaks assignable to free DMBD and $\text{Rh}_6\text{O}_{14}(\text{DPPM})$ (**3**) appeared. The DPPM in **3** could have two possible coordination forms: chelating or bridging. A preliminary X-ray diffraction study shows that it bridges two adjacent rhodium atoms of the octahedral metal cluster [11*]. It is clear from the crystal structure [12] that the two methylene hydrogen atoms of DPPM in **3** are in different environments. One is directed toward the side of the Rh triangle with a $\mu_3\text{-CO}$

Table 5

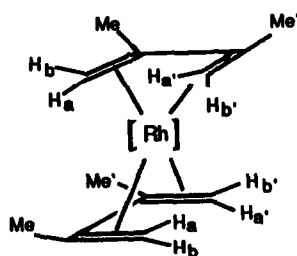
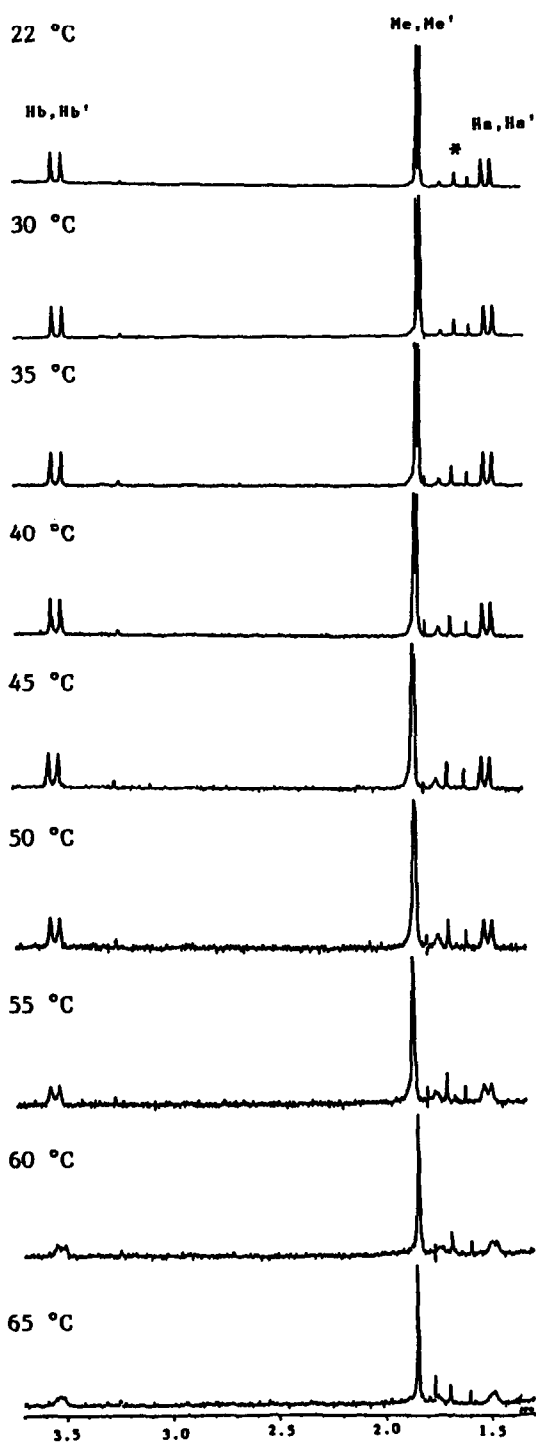
Bond lengths of the non-hydrogen atoms of **2** (esd's in parentheses)

Rh(1)–Rh(2)	2.813(1)	Rh(2)–C(22)	1.90(1)
Rh(1)–Rh(3)	2.778(3)	Rh(3)–C(31)	1.89(1)
Rh(1)–Rh(4)	2.798(1)	Rh(3)–C(32)	1.93(1)
Rh(1)–Rh(5)	2.794(3)	Rh(4)–C(41)	1.90(1)
Rh(2)–Rh(3)	2.715(3)	Rh(4)–C(42)	1.89(1)
Rh(2)–Rh(5)	2.756(3)	Rh(5)–C(51)	1.96(1)
Rh(2)–Rh(6)	2.787(1)	Rh(5)–C(52)	1.89(1)
Rh(3)–Rh(4)	2.739(3)	Rh(1)–C(11)	2.21(1)
Rh(3)–Rh(6)	2.805(3)	Rh(1)–C(12)	2.19(1)
Rh(4)–Rh(5)	2.729(3)	Rh(1)–C(13)	2.21(1)
Rh(4)–Rh(6)	2.781(1)	Rh(1)–C(14)	2.22(1)
Rh(5)–Rh(6)	2.795(3)	Rh(6)–C(61)	2.20(1)
Rh(1)–C(1)	2.23(1)	Rh(6)–C(62)	2.21(1)
Rh(2)–C(1)	2.27(1)	Rh(6)–C(63)	2.22(1)
Rh(3)–C(1)	2.10(1)	Rh(6)–C(64)	2.20(1)
Rh(1)–C(2)	2.23(1)	C(1)–O(1)	1.13(2)
Rh(4)–C(2)	2.17(1)	C(2)–O(2)	1.18(1)
Rh(5)–C(2)	2.16(1)	C(3)–O(3)	1.23(2)
Rh(3)–C(3)	2.28(1)	O(4)–O(4)	1.20(2)
Rh(4)–C(3)	2.07(1)	C(21)–O(21)	1.09(2)
Rh(6)–C(3)	2.08(1)	C(22)–O(22)	1.11(2)
Rh(2)–C(4)	2.17(1)	C(31)–O(31)	1.15(2)
Rh(5)–C(4)	2.10(1)	C(32)–O(32)	1.10(2)
Rh(6)–C(4)	2.24(1)	C(41)–O(41)	1.16(2)
Rh(2)–C(21)	1.94(1)	C(42)–O(42)	1.14(2)
C(51)–O(51)	1.11(2)	C(13)–C(16)	1.50(2)
C(52)–O(52)	1.12(2)	C(61)–C(62)	1.42(2)
C(11)–C(12)	1.42(2)	C(62)–C(63)	1.42(2)
C(12)–C(13)	1.47(2)	C(63)–C(64)	1.39(2)
C(13)–C(14)	1.40(2)	C(62)–C(65)	1.59(2)
C(12)–C(15)	1.54(2)	C(63)–C(66)	1.56(2)

Table 6

Selected bond angles of the non-hydrogen atoms of **2** (esd's in parentheses)

Rh(1)–C(1)–Rh(2)	77.4(4)	Rh(5)–C(4)–Rh(6)	80.0(5)
Rh(1)–C(1)–Rh(3)	79.8(4)	Rh(2)–C(4)–O(4)	130(1)
Rh(2)–C(1)–Rh(3)	76.6(4)	Rh(5)–C(4)–O(4)	135(1)
Rh(1)–C(1)–O(1)	133(1)	Rh(6)–C(4)–O(4)	132(3)
Rh(2)–C(1)–O(1)	130(1)	C(21)–Rh(2)–C(22)	90.5(5)
Rh(3)–C(1)–O(1)	137(1)	C(31)–Rh(3)–C(32)	91.8(6)
Rh(1)–C(2)–Rh(4)	79.1(4)	C(41)–Rh(4)–C(42)	94.3(6)
Rh(1)–C(2)–Rh(5)	79.2(4)	C(51)–Rh(5)–C(52)	98.6(6)
Rh(4)–C(2)–Rh(5)	78.3(4)	C(11)–C(12)–C(13)	119(1)
Rh(1)–C(2)–O(2)	135(1)	C(11)–C(12)–C(15)	121(1)
Rh(4)–C(2)–O(2)	134(1)	C(13)–C(12)–C(15)	120(1)
Rh(5)–C(2)–O(2)	130(1)	C(12)–C(13)–C(14)	119(1)
Rh(3)–C(3)–Rh(4)	77.9(4)	C(12)–C(13)–C(16)	122(1)
Rh(3)–C(3)–Rh(6)	80.0(4)	C(14)–C(13)–C(16)	119(1)
Rh(4)–C(3)–Rh(6)	84.4(5)	C(61)–C(62)–C(63)	118(1)
Rh(3)–C(3)–O(3)	126(1)	C(61)–C(62)–C(65)	120(1)
Rh(4)–C(3)–O(3)	133(1)	C(63)–C(62)–C(65)	123(1)
Rh(6)–C(3)–O(3)	135(1)	C(62)–C(63)–C(64)	118(1)
Rh(2)–C(4)–Rh(5)	80.2(4)	C(62)–C(63)–C(66)	122(1)
Rh(2)–C(4)–Rh(6)	78.3(4)	C(64)–C(63)–C(66)	120(1)



*: impurity

Fig. 3. Variable temperature ^1H NMR spectra of **2** in C_6D_6 .

group and the other toward the Rh triangle without bridging CO. Thus, the ^1H NMR spectra of **3** in CD_2Cl_2 showed a pair of broad quartets ($J = J_{\text{HH}} \approx J_{\text{PH}} = 12\text{--}14$ Hz) at 4.61 and 3.97 ppm, respectively, in addition to the signals in the aromatic region, indicating the non-equivalence of the two methylene hydrogen atoms of the ligating DPPM.

Reaction of **2** with two equiv. of DPPM was also complete within a few minutes and gave $\text{Rh}_6(\text{CO})_{12}(\text{DPPM})_2$ (**4**). The coordination of the DPPMs in **4** is probably bridging, since its ^1H NMR pattern is similar to that of **3**. The reaction was monitored by ^1H NMR spectroscopy, but intermediates having both DMBD and DPPM were not observed even when one equiv. of DPPM was added. Thus, substitution of the second DMBD must be rapid and the rate determining step is the displacement of the first DMBD.

In both clusters, substitution of the diene by DPPM were too fast to be determined quantitatively by NMR spectroscopy. However, it was estimated by reaction of DPPM with a mixture of **1** and **2** that the reaction of **1** was 2–3 times faster. This observation implies that the rate of diene substitution is greatly affected even by the ligands attached to the remotest rhodium apex of the octahedron.

Experimental

General methods. Infrared spectra were recorded on a JASCO A-202 IR spectrometer. ^1H NMR spectra were recorded on a JNM-GX 400 spectrometer and are reported in ppm from internal tetramethylsilane (TMS). The letter designates the multiplicity of the signals: s, singlet; d, doublet; t, triplet; q, quartet; m, multiplet; br, broad. ^{13}C NMR spectra were recorded on a JNM-GX 500 spectrometer and chemical shifts are reported relative to internal TMS. $\text{Rh}_4(\text{CO})_{12}$ was prepared by a published procedure [13]. All ligands were of the purest commercial grade and used without further purification. All reactions were carried out under argon.

Synthesis of 1 [3a] and 2. $\text{Rh}_4(\text{CO})_{12}$ (300 mg, 0.4 mmol) and 2,3-dimethyl-1,3-butadiene (DMBD) (820 mg, 10 mmol) were refluxed in hexane (10 ml) for 3 h. On evaporation of the solvent, a mixture of **1** and **2** was obtained as a brown powder. The yields of **1** and **2** determined by ^1H NMR using CH_2Cl_2 as an internal standard were 75% and 24%, respectively. Complexes **1** and **2** were separated based on their solubility difference. Addition of hexane (5 ml \times 2) to the mixture gave a solution of **2** containing a small amount of **1**, while most of **1** remained as solid. The solution was transferred to another flask by a syringe and the solvent was evaporated to give a brown solid. Extraction by hexane was repeated again. After the volume of the solution had been reduced by evacuation, slow evaporation of the solvent was conducted under a stream of argon to give dark red, prismatic crystals of **2** together with a small amount of fine cubic crystals of **1**. Since complete separation of **2** from **1** was difficult, satisfactory elemental analysis was not possible. However, a crystal of **2** suitable for X-ray crystallography was obtained from these crystals.

A smaller molar ratio of $\text{Rh}_4(\text{CO})_{12}$ to DMBD led to the preferred formation of **1**. Refluxing a 1 : 2.5 mixture of $\text{Rh}_4(\text{CO})_{12}$ and DMBD as above gave **1** in 96% isolated yield. Recrystallization from hot hexane gave dark red, cubic crystals suitable for X-ray diffraction studies.

The spectroscopic data of the products are recorded below.

$Rh_6(CO)_{14}(\eta^4-CH_2C(Me)C(Me)CH_2)$ (**1**) [7*]. 1H NMR ($CDCl_3$) δ 3.55 (d, J 1.2 Hz, 2 H), 2.18 (s, 6 H) and 1.56 (br s, 2 H); ^{13}C NMR ($CDCl_3$, only for DMBD part) δ 114.21 (d, $J(Rh-C)$ 4.6 Hz), 57.88 (d, $J(Rh-C)$ 9.1 Hz), 17.12; IR (nujol) 2120 (shoulder), 2070 (very strong), 1783 cm^{-1} (strong).

$Rh_6(CO)_{12}(\eta^4-CH_2C(Me)C(Me)CH_2)_2$ (**2**). 1H NMR ($CDCl_3$) δ 3.68 (d, J 1.2 Hz, 2 H), 3.65 (d, J 1.2 Hz, 2 H), 2.20 (s, 6 H), 2.19 (s, 6 H), 1.62 (br s, 2 H), 1.59 (br s, 2 H); ^{13}C NMR ($CDCl_3$, only for DMBD part) δ 113.90, 113.41, 57.81 (d, $J(Rh-C)$ 9.2 Hz), 57.02 (d, $J(Rh-C)$ 10.7 Hz), 17.48, 17.42; IR (nujol) 2060 (very strong), 2010 (strong), 1770 cm^{-1} (strong).

Reaction of 1 and 2 with DPPM. Complex **1** (44.5 mg, 0.04 mmol) was stirred with DPPM (15.4 mg, 0.04 mmol) at room temperature for 1 h. Brown powder was obtained after evaporation of the solvent. Recrystallization of the product from CH_2Cl_2 /hexane gave $Rh_6(CO)_{14}(DPPM)$ (**3**) [10] (50 mg, 90%) as dark red, prismatic crystals (1H NMR in CD_2Cl_2 : δ 7.15–7.75 (m, 20 H), 4.61 (br q, $J = J(HH) \approx J(PH) = 12$ –14 Hz, 1 H), 3.97 (br q, $J = J(HH) \approx J(PH) = 12$ –14 Hz, 1 H). Its unit cell parameters were obtained as described for those of **1** and **2** (vide infra). The reaction of **2** with DPPM under similar conditions gave $Rh_6(CO)_{12}(DPPM)_2$ (**4**). Its 1H NMR data in CD_2Cl_2 are as follows: δ 6.90–7.90 (m, 40 H), 4.57 (m, 2 H), 4.10 (m, 2 H), which are consistent with those of an authentic sample [10].

Reaction of a mixture of 1 and 2 with DPPM. To a CD_2Cl_2 solution of **1** (0.0017 mmol) and **2** (0.0021 mmol) in an NMR tube was added DPPM (0.003 mmol) at

Table 7

Crystal data and details of intensity collection for **1** and **2**

	1	2
FW	1091.72	1117.84
System	orthorhombic	monoclinic
Space group	$P2_12_12_1$ (No. 19)	Cc (No. 9)
a , Å	14.430(3)	17.635(2)
b , Å	16.970(3)	9.561(1)
c , Å	10.908(2)	18.234(4)
β , deg		97.24(1)
V , Å ³	2671.2	3050.0
Z	4	4
ρ (calcd), $g\ cm^{-3}$	2.296	2.377
Crystal dimensions, mm	0.14 × 0.13 × 0.12	0.19 × 0.12 × 0.11
Monochromator	graphite	graphite
Radiation ($\lambda/\text{Å}$)	Mo- K_α (0.7107)	Mo- K_α (0.7107)
Temperature, °C	20	20
2θ range, deg	4–55	4–55
Scan type	ω - 2θ	ω - 2θ
Scan speed deg min^{-1}	4.12	4.12
Indices collected	h, k, l	$h, k, \pm l$
Unique data collected	3533	7656
Reflections observed, $F_o > 3\sigma(F_o)$	2511	2929
Number of parameters refined	362	380
R	0.0425	0.0286
R_w	0.0409	0.0317
Maximum residuals, $e\ \text{Å}^{-3}$	11.8	7.3

room temperature under argon. Immediate disappearance of DPPM peaks as well as reduction of peaks due to both **1** and **2** were observed in the ^1H NMR spectra. The relative peak intensities indicated that ca. 80% of **1** and 35% of **2** had been consumed respectively. Since substitution of the second DMBD in **2** is much faster than that of the first one, displacement of the first DMBD can be considered as the rate determining step in the reaction of **2** with DPPM. Thus it was estimated from the above competitive reaction that the reaction of **1** with DPPM was 2–3 times faster than that of **2**.

Crystal structure determination of 1 and 2. Crystals of **1** and **2** were mounted in air on glass fibers. Diffraction measurements were made at 20°C on an Enraf Nonius CAD4 diffractometer in the bisecting mode employing the ω - 2θ technique and using Mo- K_α radiation. Unit cell dimensions for both crystals were obtained from least-squares refinements of the setting angles of 25 reflections with $20^\circ < 2\theta < 25^\circ$. Three reflections were monitored periodically for each structure as a check for crystal decomposition or movement, but no significant variation in these standards was observed. Absorption correction was not made because deviations of F_0 for axial reflections at $\chi \approx 90^\circ$ were within $\pm 5\%$. Both structures were solved by MULTAN [14] to locate the six rhodium atoms. The remaining non-hydrogen atoms were located from subsequent difference Fourier syntheses. All non-hydrogen atoms were refined anisotropically by the blockdiagonal least-squares method [15]. Crystal data and details of the intensity data collection are summarized in Table 7.

Lists of anisotropic thermal parameters and F_0 vs. F_c for **1** and **2** (30 pages) are available from the author (Z. H.).

References

- 1 For recent reviews on cluster catalysts see: (a) S. Otsuka and H. Yamazaki (Eds.), *Chemistry of Metal Clusters*, Gakkai Shuppan Center, Tokyo, 1986, pp. 119–196; (b) B.D. Dombek, *Adv. Catal.*, **32**, (1983) 325; (c) R. Whyman, in B.F.G. Johnson (Ed.), *Transition Metal Clusters*, John Wiley & Sons, Chichester, 1980, Chapt. 8, p. 545.
- 2 H. Yasuda and A. Nakamura, *Angew. Chem. Int. Ed. Engl.*, **26** (1987) 723.
- 3 (a) T. Kitamura and T. Joh, *J. Organomet. Chem.*, **65** (1974) 235; (b) the sole X-ray structure of rhodium cluster with diene ligand, $\text{Rh}_6(\text{CO})_{10}(\text{norbornadiene})_3$, was described only briefly, see: J. Antony, J. Jarvis, and R. Whyman, *J. Chem. Soc., Chem. Commun.*, (1975) 562.
- 4 E.R. Corey, L.F. Dahl, and W. Beck, *J. Am. Chem. Soc.*, **85** (1963) 1202.
- 5 (a) G. Ciani, M. Manassero, and V.G. Albano, *J. Chem. Soc., Dalton Trans.*, (1981) 515; (b) A. Ceriotti, G. Ciani, L. Garlaschelli, V. Sartorelli, and A. Sironi, *J. Organomet. Chem.*, **229** (1982) C9.
- 6 L. Porri, A. Lionetti, G. Allegra, and A. Immirzi, *Chem. Commun.*, (1965) 336.
- 7 ^1H NMR spectral data of **1** in CDCl_3 were incorrectly reported in the literature as follows (see ref 3a): 3.55(4 H), 2.19 (6 H) ppm, where the two proton signal at 3.55 ppm was given as a four proton signal and the peak (2 H) at 1.56 ppm was not mentioned. In fact, there was really a peak near 1.56 ppm as a shoulder of the concomitant water signal, which became clearer after the water signal was shifted to 4.67 ppm by addition of some D_2O .
- 8 R. Benn and G. Schroth, *J. Organomet. Chem.*, **228** (1982) 71.
- 9 The activation energy E_a was calculated as described previously, see: C.E. Looney, W.D. Phillips, and E.L. Reilly, *J. Am. Chem. Soc.*, **79** (1957) 6136.
- 10 D.F. Foster, B.S. Nicholls and A.K. Smith, *J. Organomet. Chem.*, **236** (1982) 395.
- 11 Unit cell parameters of **3**: a 16.649(4), b 19.002(2), c 13.830(3) Å, β 87.38(2)°, U 4370 Å³; the same as those of the known DPPM-bridging hexarhodium cluster [12].
- 12 J.A. Clucas, M.M. Harding, and S.J. Maginn, *J. Chem. Soc., Chem. Commun.*, 1988, 185.
- 13 *New Handbook on Experimental Chemistry*, Vol. 12, The Chemical Society of Japan, 1976, p. 193.
- 14 P. Main, S.E. Hull, L. Lessinger, G. Germain, J.-P. Deckerq, and M.M. Woolfson, *MULTAN* 78, University of York, York, 1978.
- 15 T. Sakurai and K. Kobayashi, *Rikagaku Kenkyusho Hokoku*, **55** (1979) 69.